Biochimica et Biophysica Acta 1798 (2010) 637–645

Contents lists available at ScienceDirect

Biochimica et Biophysica Acta

journal homepage: www.elsevier.com/locate/bbamem

Light harvesting, energy transfer and electron cycling of a native photosynthetic membrane adsorbed onto a gold surface

Gerhard J. Magis [a], Mart-Jan den Hollander [a], Willem G. Onderwaater [a], John D. Olsen [b], C. Neil Hunter [b], Thijs J. Aartsma [a], Raoul N. Frese [a,*]

[a] Biophysics, Faculty of Mathematics and Natural Sciences, Leiden University, P.O. Box 9502, 2300RA Leiden, The Netherlands
[b] Department of Molecular Biology and Biotechnology, University of Sheffield, Sheffield, S10 2TN, UK

ARTICLE INFO

Article history:
Received 24 September 2009
Received in revised form 17 December 2009
Accepted 21 December 2009
Available online 28 December 2009

Keywords:
Photosynthetic membrane
Rhodobacter sphaeroides
Supramolecular organization
Confocal spectroscopy
Light-induced electrochemistry
Energy transfer
Electron transfer
Light-harvesting complex
Reaction center complex

ABSTRACT

Photosynthetic membranes comprise a network of light harvesting and reaction center pigment–protein complexes responsible for the primary photoconversion reactions: light absorption, energy transfer and electron cycling. The structural organization of membranes of the purple bacterial species *Rb. sphaeroides* has been elucidated in most detail by means of polarized light spectroscopy and atomic force microscopy. Here we report a functional characterization of native and untreated membranes of the same species adsorbed onto a gold surface. Employing fluorescence confocal spectroscopy and light-induced electrochemistry we show that adsorbed membranes maintain their energy and electron transferring functionality. Gold-adsorbed membranes are shown to generate a steady high photocurrent of 10 $\mu A/cm^2$ for several minutes and to maintain activity for up to three days while continuously illuminated. The surface-adsorbed membranes exhibit a remarkable functionality under aerobic conditions, even when exposed to light intensities well above that of direct solar irradiation. The component at the interface of light harvesting and electron cycling, the LH1 complex, displays exceptional stability, likely contributing to the robustness of the membranes. Peripheral light harvesting LH2 complexes show a light intensity dependent decoupling from photoconversion. LH2 can act as a reversible switch at low-light, an increased emitter at medium light and photobleaches at high light.

1. Introduction

Photosynthetic membranes are compartmentalized cellular structures containing the solar-energy transducing machinery. The most abundant protein complexes constituting this machinery are light-harvesting (LH) complexes, which are responsible for the absorption of sunlight and subsequent excited state energy transfer, and reaction centers (RC), where the energy is utilized to initiate the primary charge-transfer reactions [1]. Because of their relative simplicity, the photosynthetic membranes from purple bacteria have been characterized in detail by near infrared (NIR) spectroscopy and, more recently, by atomic force microscopy [AFM, 2–6]. The purple bacterium *R. sphaeroides* synthesizes vesicle-shaped membranes, or chromatophores, that contain two types of LH complexes, the peripheral LH2 complex and the LH1 complex that surrounds the RC complex. The RC-LH1-PufX complexes of *R. sphaeroides* form a dimeric supercomplex that forms extended linear arrays in the native membranes. The polypeptide PufX has been shown to be the determinant factor for RCLH1 dimerization [7–10]. In the wild-type (WT) photosynthetic membrane, these linear arrays are interspersed by LH2 complexes [6]. In conjunction with structural models of the LH and RC complexes, and data from polarized light-spectroscopic measurements on intact membranes, a detailed description of the supramolecular organization of *R. sphaeroides* membranes has been developed [5,11]. Similar investigations on *R. sphaeroides* mutant membranes with altered composition (monomeric RC-LH1 and LH2) showed that packing effects reminiscent of colloidal systems, rather than specific protein–protein interactions, are a driving force for the observed supramolecular organizations [12]. In the case of *R. sphaeroides* and other species, AFM images revealed a close packing of the photosynthetic components which is a prerequisite for a highly efficient energy transferring network. Nevertheless such images do raise the question whether these native membranes are still capable of performing their energy transducing function upon adsorption to a solid support, or if the isolation and adsorption have an adverse effect. Surface-adsorbed photosynthetic membranes have not been characterized functionally before. A functional assessment comprises the light absorbing and subsequent energy transferring mechanisms as well as the ability for electron cycling. These functions can be probed by means of confocal spectroscopy and light-induced electrochemistry [13,14]. The latter technique is facilitated by the attachment of a preparation onto a conducting surface that serves as an electrode to or

* Corresponding author.
E-mail address: frese@few.vu.nl (R.N. Frese).

0005-2736/$ – see front matter © 2009 Elsevier B.V. All rights reserved.
doi:10.1016/j.bbamem.2009.12.018

from which electrons can be channeled; typically, this electrode consists of gold. This technique has been applied on several photosynthetic complexes, which were either engineered for a specific attachment or adsorbed via functionalized groups on the surface [15–19]. In all these cases surface-immobilization of the complexes involved functionalized gold surfaces using self-assembled monolayers (SAM's) with specific terminal functionality. In contrast, we recently observed the possibility of directly adsorbing isolated RC complexes onto a bare-gold electrode without functionalisation of the surfaces or the proteins (Frese RN. den Hollander MJ, Jones MJ and Aartsma TJ; unpublished results). Moreover, applying an external potential within the range of the open circuit potential of the RC and charge carriers, i.e. cytochrome *c* (cyt-*c*) and extrinsic quinones (Q-0), light-induced currents could be observed under ambient conditions. Here we present a study by light-induced electrochemistry and confocal spectroscopy on native membranes of *R. sphaeroides* adsorbed directly onto a solid gold support. In contrast to mica or glass, we find that intact chromatophore vesicles adhere as a flattened structure onto gold, withstanding rinsing and drying steps. Wavelength dependent fluorescence excitation and current action spectra indicate that these untreated, wild-type (WT) chromatophores adsorbed on gold retain their energy- and electron transferring capabilities. Surprisingly, membranes remain functional under aerobic conditions. Fluorescence emission and excitation spectra were obtained under similar conditions. In all cases, we find that all three pigment–protein complexes responsible for the primary photoconversion reactions remain functional, although a decreased contribution of the peripheral LH2 complex is observed. This decrease as well as the possibility for reversibility showed to be variable with light illumination intensity. Results are compared with photosynthetic preparations in solution and purified LH1 adhered onto a surface. Our work shows the feasibility of coupling photo-active biological systems to non-biological surfaces, with retained functionality when exposed to relatively intense light and to air.

2. Materials and methods

2.1. Biological membranes

Wild-type cells of *R. sphaeroides* NCIB 8253 were grown photosynthetically at intermediate light intensity (500 W m^{-2}) for 18–20 h. Cells were disrupted through ultra-sound sonication and subsequently loaded onto a sucrose gradient. The gradient was spinned for 20 h and the red colored band was isolated.

2.2. RCLH1 membranes

Cultures were grown semi-aerobically in a shaker incubator at 34 °C and 180 rpm. The cells were pre-treated with 2 mL of 10 mg/mL lysozyme (Sigma Chemicals) for 30 min on ice and then lysed by two passages through a French Press at 18,000 psi. The resulting lysate was treated with DNAse to digest the genomic DNA prior to loading onto a 15/40% w/w sucrose (in 10 mM HEPES pH 7.5, 1 mM EDTA, 1 mM DTT buffer) discontinuous gradient and centrifugation at 27 krpm for 10 h. The pigmented membranes were harvested from the 15/40% interface and frozen at −20 °C until use.

2.3. Isolated photosynthetic complexes

LH2 membranes were solubilised by the addition of β-OG to a final concentration of 2.5% and stirring for 30 min at 4 °C. The solubilised membranes were applied to a pre-equilibrated DEAE sepharose column (Sigma Chemicals) and washed extensively with increasing concentrations of NaCl for a minimum of 90 min. The purified protein was eluted from the column using a 150–400 mM NaCl gradient over 60 min and 4 mL fractions were collected. The elution profile showed two peaks of which the second peak was demonstrated by EM analysis to consist of monodisperse LH2 complexes. These fractions were then used in all subsequent experiments. The preparation of the LH1-only purified complexes was identical except for the use of the detergent β-DDM. During solubilisation β-DDM was added to a final concentration of 1% and all the columns were run at a concentration of 0.03% β-DDM.

2.4. Gold-surface preparation

A 1 nm adhesion layer of molybdenum germanium (MoGe) was first sputtered on mica using an ATC-1800 magnetron sputtering system with a deposition rate of 1.32 nm/min (10 mTorr Argon environment). On top of this 20 nm thick gold films were sputtered with a deposition rate of 9.2 nm/min (5 mTorr environment composed of a mixture of Argon with 1% oxygen). This resulted in gold films with a typical RMS roughness of 0.3 n.

2.5. Protein immobilization for spectroscopy

2.5.1. Attachment of purified LH1 on gold

25 μL of bulk LH1 solution (OD_{870} 2–3 in a buffer containing 10 mM HEPES (pH 8), β-DDM (0.03%), 150 mM NaCl and 10 mM DTT) was diluted with 175 μL buffer (10 mM HEPES (pH 8) and β-DDM (0.03%)) and loaded on the surface. After 15 min incubation the sample was rinsed with 1 mL of buffer. This loading and rinsing were repeated 2 times after which the surface was gently blown dry under a mild stream of nitrogen gas.

2.5.2. Attachment of WT chromatophores on gold

A 50 μL sample was loaded on the gold surface and left to incubate for 30 min. After this the surface was rinsed with 1 mL of buffer (10 mM HEPES at pH 7.5–8) and gently blown dry under a mild stream of nitrogen-gas.

2.6. Atomic force microscopy

Atomic force microscopy (AFM) images of the samples were obtained using a commercial AFM (Nanoscope IIIa, Veeco, Santa Barbara, CA, USA). Tapping mode images in air were acquired with an E-scanner (14 μm range) and using Si probes with a resonance frequency of 75 kHz and a nominal spring constant of 2.8 N m^{-1}.

2.7. Spectroscopy

2.7.1. Confocal fluorescence spectroscopy

Experiments were performed at room temperature with a home-built confocal microscope setup with the objective mounted inside a cryostat. The latter enables measuring in an air free environment by vacuum pumping the cryostat. Homogeneity of the sample distribution on the surface was checked by confocally scanning the laser over a wide-range (hundreds of micrometers) at a fixed excitation wavelength (800 or 850 nm for LH2, 870 nm for LH1) and monitoring the fluorescence signal using an avalanche photodiode (APD, Perkin-Elmer SPCM-AQR-16).

Fluorescence emission spectra were recorded by directing the emitted fluorescence via a series of long-pass filters with a transmission between 815 and 1015 nm (Hugo Anders, Germany), towards a blazed grating (Richardson Gratings) that disperses the collimated fluorescence. A lens is finally used to project the diffracted beam onto a liquid-nitrogen-cooled CCD camera (Roper Scientific, USA). The excitation intensity used to record an emission spectrum was 200 W cm^{-2} or as indicated in the text. Integration times were typically 60 s. The recorded spectra were all corrected for the sensitivity of the CCD camera.

Fluorescence excitation spectra were recorded in vacuum at room temperature, unless otherwise stated. A series of 3 identical interference

band pass filters was employed in the detection path to remove most of the stray light (residual excitation light passing through the detection-filters). Two sets of filters were used depending on the sample under investigation, one with a transmission between 875 and 910 nm (for purified LH2 measurements), and the other with a transmission between 905 and 940 nm (for purified LH1 and membrane measurements). Excitation spectra were recorded by scanning the wavelength of the titanium sapphire (TiSa) laser from 790 nm (lower limit of the laser) to either 870 or 900 nm, depending on which filter-set is used.

2.8. Photostability measurements

2.8.1. On a surface

The scheme for fluorescence emission spectroscopy as mentioned above was employed with the exception that the long-pass filters for emission detection are replaced by a series of 3 identical interference band pass filters (transmission between 875 and 910 nm for LH2, transmission between 905 and 940 nm for LH1). This limits the detection of the emission to the red part of the fluorescence, but the main advantage of this scheme is that we can now excite LH1 at a longer wavelength where the complex has more absorption. The detected fluorescence signal was integrated for 60 s.

2.8.2. In solution

Samples were diluted in the appropriate buffer to an OD of 0.1 before loading into the cuvette. The cuvette has a volume of 60 μL and during the photostability measurements in solution approximately half of this volume was illuminated. Measurements were conducted on a home-built setup integrating a spectrophotometer (Ocean Optics, QE6500) for absorbance measurements and fluorescence detection (cut-off filter transparent at 700–1000 nm, and a halogen lamp for long-term illumination (400–1000 nm) and excitation (cut-off filter transparent at 400–700 nm). The power of the white light was 135 mW cm^{-2} on the cuvette open to air. Long-term illumination (and excitation) light was passed through a 10 cm water-filter to prevent heating. The samples were continuously illuminated until no reduction in absorption or emission was observed.

2.9. Electrochemistry

The bare-gold working electrode was cleaned prior to use by sonicating and rinsing with purified water and subsequent grinding. A drop of 10 μL of solution containing membrane was deposited onto cleaned bare-gold electrodes and left to incubate for 1 h in the dark at 277 K. Subsequently, the electrodes were rinsed 3 times with 3 mL 10 mM phosphate buffer, inserted into a home-built cell, and immersed in the measuring buffer (volume approximately 7 mL). The buffer solution contained 20 μM horse heart cytochrome *c* (Sigma, 97% purity) and 100 μM Q-0 (or 2,3-dimethoxy-5-methyl-1,4-benzoquinone, Aldrich, 99% purity). The potential was set at a specific value and the whole system was left to equilibrate in the dark until the dark current reached a typical value of a few nano-amperes. We then switched on the light and measured the response in current, after which the light was switched off again. Electrodes and potential were controlled by a commercial potentiostat from CHI-instruments with the standard three-electrode configuration: a working electrode on which the membranes were deposited, a platinum counter electrode to measure the current and a reference electrode with a fixed potential relative to which the potential was set. The reference electrode was a standard calomel electrode (SCE): KCl saturated (Hg/Hg_2Cl_2) electrode. Illumination was accomplished by light from light emitting diodes (LEDS), with a broadband excitation at 870 nm (approximately 50 nm FWHM) or by a home-built halogen lamp-monochromator design. Wavelength dependent action spectra were obtained from step-wise scanning the monochromator design with a computer-controlled shutter.

3. Results and discussion

3.1. Adsorption of membranes onto a gold surface

Isolated *R. sphaeroides* membranes were directly deposited onto a gold surface or gold-electrode or mica surface. The preparations were left to incubate in the dark for 30 min to 1 h at 277 K and subsequently rinsed with buffer solution and blown dry with a gentle flow of nitrogen gas. A comparison of the adsorption of untreated membranes on mica and gold obtained by low-resolution atomic force microscopy (AFM) is shown in Fig. 1. Panel a shows the isolated membranes adsorbed onto mica. A range of high semi-spherical shapes (height 20 to 70 nm, width between 100 and 700 nm) can be observed, reminiscent of collapsed spherical chromatophores as well as larger structures as observed before in electron microscopy images [20]. The larger structures are a consequence of the simple purification procedure, designed to isolate photosynthetic membranes with minimal disturbance. Panel B shows similarly prepared membranes on a mica surface covered with a 20 nm layer of gold. Great care was taken to produce a uniformly flat gold surface ($\approx$ 0.3 nm surface roughness) for easy identification of adsorbed structures by scanning probe techniques. The height profile of such an image shows uniformly flat, singular membranes of about 7 nm in height and 100–200 nm in diameter, dimensions which are similar to fragments of detergent-treated membranes are adsorbed onto mica for high-resolution AFM imaging [6]. We investigated several methods of membrane adsorption to the mica and gold surfaces. We either consecutively replaced the liquid droplet containing membranes by buffer or rinsed the surfaces with buffer. In all cases the mica surface showed larger structures compared to the gold surface. It appears that chromatophores retain their intact vesicular structure more upon adsorption to mica, whereas they open up, or rupture to form single membrane bi-layers when they adsorb onto gold. This disruption might be caused by strong attractive forces between the gold and the vesicular membranes, sufficient to overcome the native forces that determine the shape of the vesicles.

3.2. Electron-transfers of photosynthetic membranes adsorbed onto a gold-electrode

A membrane-covered gold-electrode was immersed in buffer solution, which contained cytochrome *c* (*cyt-c*) and extrinsic quinones (Q-0) as electron carriers. The light-induced current action spectra and absorbance of the chromatophores in buffer solution (crosses) are shown in Fig. 2a. Current action spectra are obtained by measuring light-on light-off traces at 5 nm wavelength intervals, upon illumination by the output of a scanning monochromator with a tungsten light source. We found that maximum current is generated at a potential of −100 mV (referenced to a standard calomel electrode or SCE). At this potential the electrons flow from the gold to reduce the RCs, either directly or with cyt-c as mediator, while current cycling is enabled via Q-0 towards the counter electrode [15,16]. The wavelength dependent current action spectrum (black squares) closely follows the absorbance bands of the chromatophores. Both spectra are dominated by the most abundant light-harvesting complex LH2, which absorbs around 800 nm and 850 nm. The other light-harvesting complex LH1 appears as a pronounced shoulder at 870 nm. The electron transferring reaction center complex, which is responsible for the light-induced current, is not visible in both spectra since the absorbance is much smaller compared to the LH complexes. We conclude that the light absorbed by all components within the membranes contributes to the induced current. Clearly, these membranes remain functional while adsorbed onto a gold-electrode.

The induced photocurrent and the absorbance spectrum did not completely match, however, and therefore we inspected the light-intensity dependence of current generation. In Figs. 2a and b, measurements of light-induced currents from native membranes are

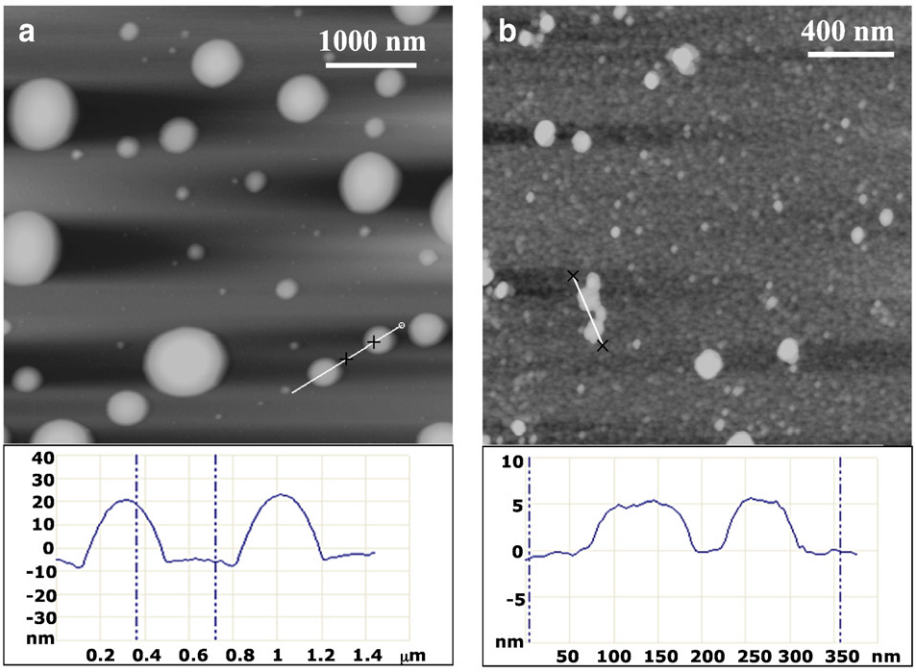

Fig. 1. Tapping mode AFM images in air of membranes adsorbed onto a mica and gold surface. (a) AFM topography image of isolated WT chromatophores adsorbed on a mica surface (top panel) and height profile along the white line (bottom panel). Grey scale 70 nm. (b) AFM topography image of WT chromatophores adsorbed on a gold substrate (top panel) and height profile along the white line (bottom panel). Grey scale 12 nm. White lines in the topography images indicate the lines along which the height profiles are measured; the crosses in the topography images correspond to the dash-double dot lines in the height profiles.

shown as a function of illumination power (represented as percentage of maximum illumination). In order to show the contribution of the LH-systems relative to the RCs, the absolute currents (Fig. 2b) were normalized at 750 nm, where two intrinsic RC pigments, bacteriopheophytins, dominate absorption (Fig. 2a). The effect of higher illumination power is striking: more light results in a higher photocurrent (Fig. 2b) but with a strong decrease in contribution from the LH2 complexes relative to the RCs (Fig. 2a). At the lowest power at which we can measure a photocurrent, LH2 does not contribute fully to the action spectrum (black squares). At highest illumination, also LH1 appears not to fully contribute to the photocurrent. At this illumination intensity the correspondence between the current action spectrum and the absorbance is lost. Here the spectral signature of the LH complexes is lost and mostly RCs appear to generate currents. We note that the change of the current action spectrum upon changing the illumination intensity is fully reversible, which shows that this effect is not caused by photobleaching.

We find no indication that saturation effects occur, because within the illumination regime where LH2 contribution can be observed, the induced current is proportional with light intensity; the slight deviations may be due to non-homogeneous illumination at different powers. Moreover, as discussed in more detail below, broadband illumination results in much higher currents, indicating the absence of limiting factors concerning electron transfers within the gold-membrane-buffer system.

We also investigated membranes of a mutant strain that contains only RC–LH1 complexes, without LH2 or PufX. The absorbance and action spectra (Fig. 2c) are dominated by the LH1 complex, with small RC bands visible at 800 nm and 750 nm. For this preparation the light-dependent current closely matched the absorbance spectrum at 20% of the maximum illumination intensity. Upon further increase of the intensity the contribution of LH1 to the photocurrent decreases similarly as for the LH2 component within WT membranes (Fig. 2a). Generally, the contribution of LH1 to the photocurrent is similar in RC-LH1-only and WT membranes.

Our photocurrent data suggest a light-dependent decoupling of the light-harvesting complexes to further energy transfer or photoconversion mechanisms. Light-induced decoupling starts off at a light intensity below our experimental limit (~150 µW/cm^2 at 870 nm) in the case of LH2, and between 3 and 7 mW/cm^2 at 870 nm for LH1. At maximum intensity (15 mW/cm^2 at 870 nm) LH2 does not participate significantly in photocurrent generation, while approximately 20% of LH1 still contributes.

For both the RC-LH1 mutant and WT membranes, the addition of cyt-*c* proved to be essential in order to achieve high (>5 nA) photocurrents (data not shown). Cyt-*c* has been shown to act as a molecular relay between RCs and the electrode to enhance electron transfer [15]. Since membranes are large and curved structures, an unequal distance between many RCs and the electrode is expected and thus the necessity for cyt-*c* as a mediator.

In Fig. 2d we show the result of testing the photostability of the native membranes towards current generation under continuous illumination, while exposed to air. Using a broadband LED (FWHM 50 nm) centred at 850 nm for illumination we achieve an initial photocurrent of 10 µA/cm^2. This current did not show a significant decrease for several minutes (in terms of the induced current, LED illumination was equivalent to 870 nm single-wavelength excitation at 20 mW/cm^2 or 0.5 µmol photons/m^{2}s). This represents the highest photocurrent per illumination photon from a photosynthetic material adsorbed onto an electrode to date. During three days of illumination under aerobic conditions, membranes sustain a significant photocurrent. At the end of this experiment the residual light-induced current was approximately 0.5% of the initial value (see inset). In total, during these three days 10 to 17 mC of charge was transferred by photoconversion in the membranes. Since there is also LH2 present in at least a 1:3 ratio, this would imply for a fully covered electrode a lower limit of on average 5×10^6 turnovers per RC, or one electron cycled through the gold-membrane-buffer system every 50 ms. Part of the electrode may well be uncovered and many RCs may well be unfavourably positioned for electron transfer, therefore the real average number of turnovers per RC is likely much higher.

We conclude here firstly that WT chromatophores and RCLH1-only mutant membranes remain functional while adsorbed onto a bare-gold electrode, under aerobic conditions. Currents can be generated

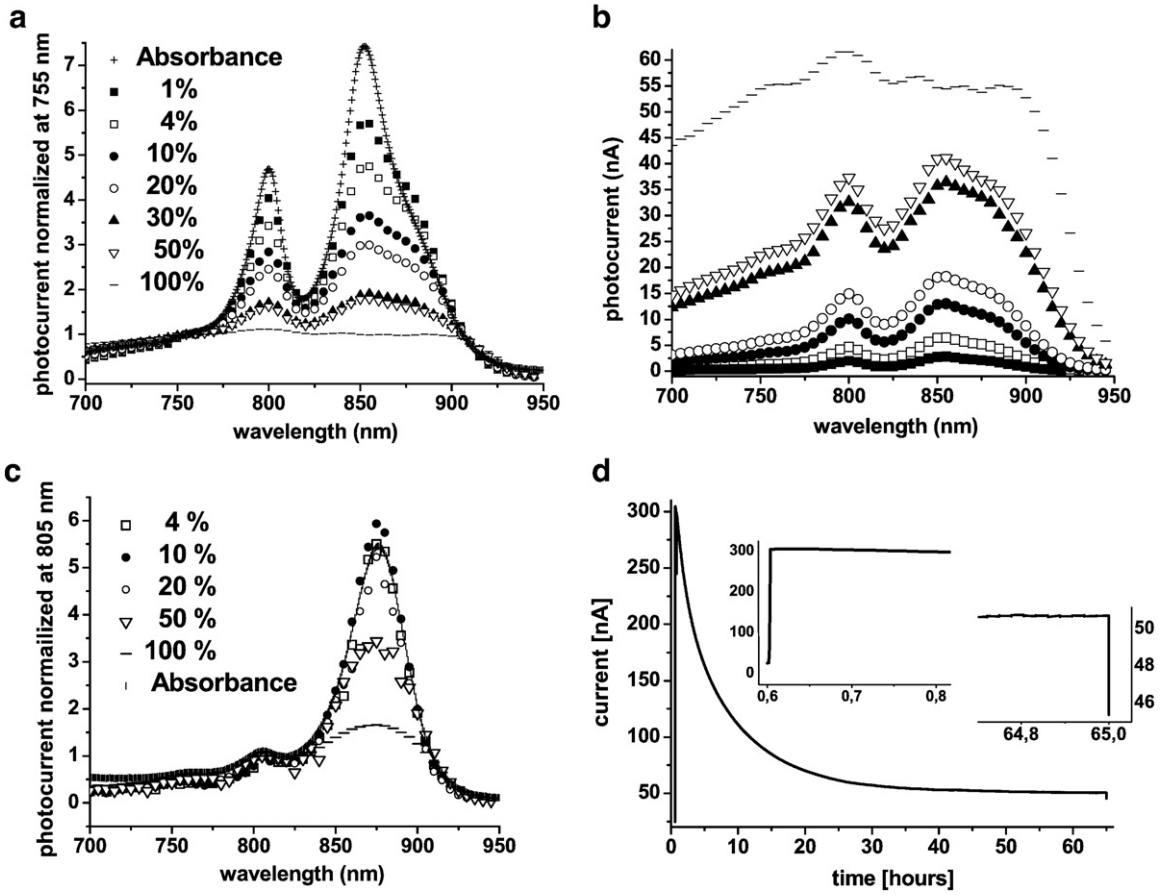

Fig. 2. Absorbance and light-induced-current action spectra of membranes adsorbed onto a gold surface. (a) Light-induced current action and solution absorbance spectra from WT chromatophores. Illumination powers indicated as percentage of maximum (100%) illumination that is 15 mW cm^{-2}; spectra normalized at 750 nm. (b) Absolute light-induced currents from WT chromatophores with illumination powers as in panel a. (c) Light-induced current action and solution absorbance spectra from RCLH1 mutant membranes. Illumination powers as in Fig. 1a; spectra normalized at 805 nm. (d) Light-induced current during continuous illumination with a LED centred at 850 nm, $V = -100$ mV vs. SCE. Inset: magnifications of the first and last 10 min of the light-induced current. At 0.6 h the light was turned on and after 65 h the light was turned off.

continuously for up to three days. Last, higher illumination intensity reduces the light harvesting contribution to the photocurrent.

3.3. Energy-transfer and photostability of photosynthetic membranes adsorbed onto a gold surface

The previous measurements indicated that on a gold surface, native vesicular shaped membranes open up spontaneously upon adsorption, without specific chemical treatment. To determine the intrinsic photostability of the system, we performed a spectral analysis of the gold-adsorbed membranes by confocal fluorescence excitation and emission spectroscopy. Fluorescence excitation spectra report on energy transferring capabilities of the complexes in the membrane, i.e. B800→B850 and LH2→LH1 transfer. Fluorescence emission spectra serve to indicate the photoactivity under various experimental conditions (vacuum, aerobic, and high illumination power). WT chromatophores were prepared and adsorbed onto a gold surface similarly as for the previous electrochemistry measurements. Excitation and emission spectra of such preparations are compared to spectra of the same preparations in buffer solution. Fluorescence excitation spectra were obtained by scanning the excitation laser from 780 to 900 nm. Emission was detected between 905 and 940 nm. The power of the laser could be attenuated from 200 nW to 7 mW, which corresponds to a light intensity focused on the sample by a microscope objective of 20 W cm^{-2} (lowest) to 637 kW cm^{-2} (highest); note that the typical power for single-molecule spectroscopy is about 1 kW cm^{-2}.

In Fig. 3a we compare the absorbance of isolated membranes in solution and fluorescence excitation spectra of gold-adsorbed membranes in vacuum. We observe all three light-absorbing components within the membranes; originating from LH2, with bands centred at 800 nm and 850 nm, and LH1, centred at 870 nm. Since excitation spectra are measured at the emission wavelength of LH1, the excitation spectrum shows that intra-LH2 and LH2→LH1 energy transfer is retained. The excitation spectrum does appear to have a slightly larger width compared to the absorption spectrum in solution, which may be either due to normalization at 850 nm which does not take any loss of absorbance or emission into account or an increased disorder upon adsorption. Also the gold surface may interact more strongly with the B850 BChl's but such effect is not expected since we probe far off-resonance with the plasmon bands of gold. The gold surface is likely a decay channel for excitations though, quenching through direct dipole couplings, which may be tuned by the dielectric of the proteins. Because we do not observe a significant mismatch between the contribution of LH2 and LH1 to the excitation spectrum, quenching appears not to be different for LH2 and LH1.Together with the previous photocurrent data, this measurement shows the functional adsorption of unprepared membranes onto gold.

We continued by investigating the functioning of the membranes towards higher illumination intensities. In Fig. 3b, upper panel, we show the effect of changing illumination power from 20 to 2750 W cm^{-2}, (referred to as low- and high power in this paragraph, respectively). We observe a decrease of the fluorescence excitation signal. The lower panel shows the difference between high and low-power spectra. The lineshape of the difference signal indicates a decreased contribution of LH2 for the high-power excitation spectrum. Fig. 3c shows the fluorescence emission spectra for the same two illumination powers.

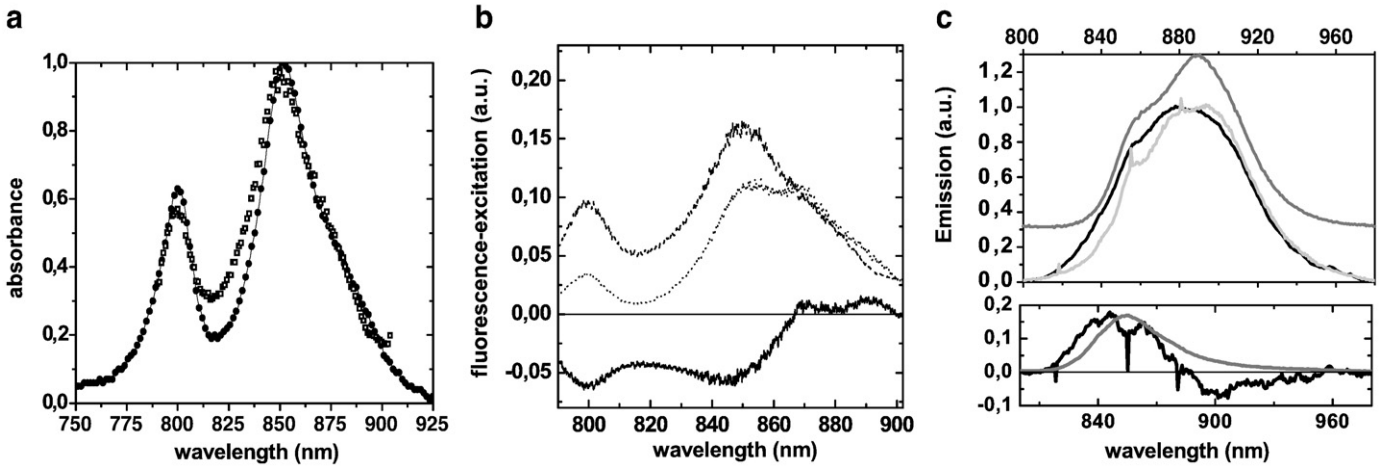

Fig. 3. Fluorescence spectra of WT chromatophores on a gold substrate and solution. (a) Isolated WT chromatophores: normalized absorbance in solution (open squares) and fluorescence excitation on a gold surface (black circles); excitation spectrum acquired in vacuum at 20 W cm^{-2}, emission detected between 905–940 nm. (b) Fluorescence excitation spectra in vacuum of WT chromatophores on gold with different excitation intensities: high power 2750 W cm^{-2}, dotted curve) and low power 20 W cm^{-2}, dashed curve). The spectra were normalized with respect to the excitation intensity. The solid line shows the difference spectrum (high power minus low power). Emission detected between 905 and 940 nm. (c) Fluorescence emission spectra in vacuum of WT chromatophores on gold recorded with high- (light grey) and low-power (black) illumination and in solution (dark grey). The spectra were not normalized but both scaled to excitation power. Lower panel: difference spectrum of the emission spectra (high power minus low power; black line). Excitation on gold at 800 nm, in solution broad illumination range: 400–600 nm. The solid grey line shows the fluorescence emission of isolated LH2 complexes.

Spectra were not normalized but scaled to the illumination power. Emission spectra closely resemble the emission from WT chromatophores in solution (Fig. 3c, upper trace). The low-power emission band is smaller on the blue side compared to the high illumination emission. Fig. 3d shows the difference between the two emission spectra and a comparison with emission of purified LH2 complexes. The two signals are spectrally similar, indicating an increase of LH2 emission for high-power illumination. The increased LH2 emission is concomitant with the decreased contribution of LH2 to the high intensity excitation spectrum in Fig. 3b. Since we detect the excitation signals as LH1 emission this implies that at high-power illumination energy transfer between LH2 and LH1 is reduced, consistent with an increased LH2 emission, and not for instance by LH2 photobleaching. We find similar effects for chromatophores in solution under prolonged white light illumination (not shown); in both cases these were not immediately reversible. Although an increased emission of LH2 may well explain the decoupling of LH2 to current generation as shown in the electrochemistry measurements, the differences in illumination powers applied do not allow a direct comparison between the two types of experiments.

Our photocurrent data showed the functionality of the gold-adsorbed membranes under aerobic conditions. We therefore compared the adsorbed native membrane assemblies under aerobic and vacuum conditions. We also investigated the effect of higher intensity illumination at 800 nm and 850 nm, probing mainly LH2 and both, LH2 and LH1, respectively. Fig. 4 shows the results on the excitation and emission spectra for anaerobic and aerobic conditions and the effects of high-power illumination. In Fig. 4a three fluorescence excitation spectra in vacuum are shown. The initial spectrum of the native chromatophores (dotted curve, 150 W cm^{-2}), shows contributions from both LH2 (800 and 850 nm) and LH1 (875 nm). Also here we observed a decreased contribution of LH2 to the excitation spectrum relative to LH1, similar as in Fig. 3b. We observe significant bleaching (on a time scale of minutes) only when illuminating the sample at maximum laser output. After exposing the sample for 5 min to 800 nm light, at an intensity of 637 kW cm^{-2}, a decreased contribution of LH2 of 60% and LH1 of 15% of the initial peak value can be observed (solid line). A consecutive third spectrum was acquired after 5 min irradiation with 850 nm light, at 443 kW cm^{-2} (dashed curve). This results in a further reduction for both the B850 LH2 and LH1 signals and a minor effect on LH2 B800. A slight peak is observed at 890 nm of unknown origin, either it represents an effect of photobleaching or it may be emission leaking through the filters.

Light-irradiation dependent emission spectra of native membranes are shown in Fig. 4b. Emission spectra were obtained with excitation at 150 W cm^{-2}, in between spectral measurements the sample was exposed to high light intensities. In vacuum (left panel) we measure a 10% reduction in emission after irradiating the membranes for 5 min at 800 nm with 50 kW cm^{-2}. Only after prolonged irradiation (see legend for details) stronger photobleaching effects are observed. In air (right panel), we detect stable fluorescence emission at an illumination power of 150 W cm^{-2} (solid line). In fact, also at higher light-irradiation intensities we did not observe immediate photobleaching of LH1 or LH2 components. We illuminated membranes at 800 nm (5 min, 50 kW cm^{-2}, dotted line) and at 850 nm (30 min with 75 kW cm^{-2}, dashed line). Each measurement was performed on a fresh spot of the sample. We observed a gradually decreasing emission signal in time, down to 35% (800 nm excitation) and 15% (850 nm excitation) of the initial emission counts. A slight blue or red shift of emission maximum can be observed depending on the irradiation wavelength, indicating selective photobleaching of LH2 and LH1.

Our data show functional energy transfers and absence of photobleaching for gold-adsorbed membranes up to 2000 W cm^{-2} under anaerobic and 150 W cm^{-2} under aerobic conditions. It took several minutes of high-power illumination before LH-systems started to become inactivated. But also at these high powers significant amounts of LH1 and LH2 remained photoactive, both in vacuum and under ambient conditions. LH2 complexes appear to be more easily photodeactivated compared to LH1, first by decoupling energy transfer to LH1 under moderate intensities, then by photobleaching at higher intensities.

3.4. Photostability of isolated light-harvesting complexes

Results discussed in the previous section demonstrated the exceptional stability of the light-harvesting systems, even under aerobic conditions, when embedded within a membrane. These results are in stark contrast to many previously reported single-molecule experiments [21]. A large body of work exists on single-molecule fluorescence of the LH2 complex and all data confirm the rapid, irreversible photobleaching of this complex under aerobic

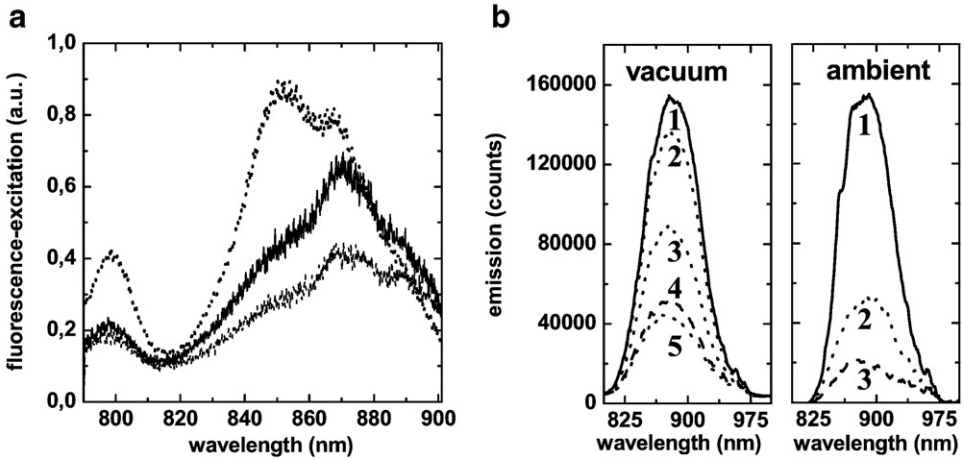

Fig. 4. Fluorescence spectra of WT chromatophores on a gold substrate. (a) Fluorescence excitation spectra in vacuum of WT chromatophores before illumination (dotted curve), after illumination at 800 nm for 5 min with an intensity of 637 kW cm^{-2} (solid curve), and after illumination at 850 nm for 5 min with 443 kW cm^{-2} (dashed curve). All excitation spectra were taken with an approximate excitation intensity of 150 W cm^{-2},emission detected between 905 and 940 nm. (b) Fluorescence emission spectra of WT chromatophores in vacuum (left panel) and under aerobic conditions (right panel) by exciting at 800 nm with 50 kW cm^{-2}; integration time of 3 s. Left panel: Between spectra 1 and 2 the sample was illuminated for 5 min with 50 kW cm^{-2} at 800 nm. Between 2 and 3 the sample was illuminated with this same power for 30 min. Between 3 and 4 the sample was illuminated with 637 kW cm^{-2} for 30 min. Between spectra 4 and 5 the shutter was closed for 30 min to measure the recovery of the sample. Right panel: Between spectra 1 and 2 the sample was illuminated with 50 kW cm^{-2} for 5 min at 800 nm. Between 2 and 3 a new spot of the sample was illuminated with 75 kW cm^{-2} for 30 min at 875 nm.

conditions [22]. Membranes are assemblies of protein complexes, forming an energy transfer network of hundreds of complexes, which in principle facilitates efficient energy dissipation even when some components are photobleached. From this viewpoint it is interesting to compare the photostability of the membrane-embedded pigment–protein complexes with that of isolated LH2 and LH1.

Fluorescence excitation and emission of isolated, detergent-solubilized LH1 and LH2 were measured under ambient conditions. Results on isolated LH1 and LH2 complexes bound onto a gold surface via engineered cysteine residues or mediated through self-assembled monolayers will be reported elsewhere. In all cases, the emission of isolated LH2 adsorbed on gold or other surfaces under aerobic conditions decreased within seconds to zero. LH1, most surprisingly, was much more stable under aerobic conditions. Fig. 5a shows the excitation and emission spectra of WT LH1 complexes directly adsorbed onto a bare-gold surface and the emission counts at maximum obtained at various intervals of prolonged light irradiation. AFM images indicated the presence of approximately 100 well-separated, LH1 complexes within a focal spot (not shown). The excitation and emission spectra closely resemble LH1 solution spectra, showing no adverse effect on the structural and electronic configurations upon gold-adsorption. Irradiating LH1 for 6 consecutive hours with illumination powers of 73 to 647 W cm^{-2} only caused a few percent drop in LH1 emission. The superior photostability of LH1 is most clearly demonstrated by the fact that it required 10 to 15 h of continuous irradiation with an intensity of 228 kW cm^{-2} to finally reduce the emission of LH1 down to 20% of the initial level.

Similar measurements were conducted on isolated LH1 complexes adsorbed onto a glass surface and again a steady emission signal was observed with high photostability (not shown). We also probed the stability of LH complexes dissolved in buffer solution under continuous white-light illumination. Also in this case the rate of photobleaching of LH2 was, as measured by emission intensity, 2 orders of magnitude faster than for LH1 (Fig. 5b). During this procedure, no significant change in the absorption spectra could be detected.

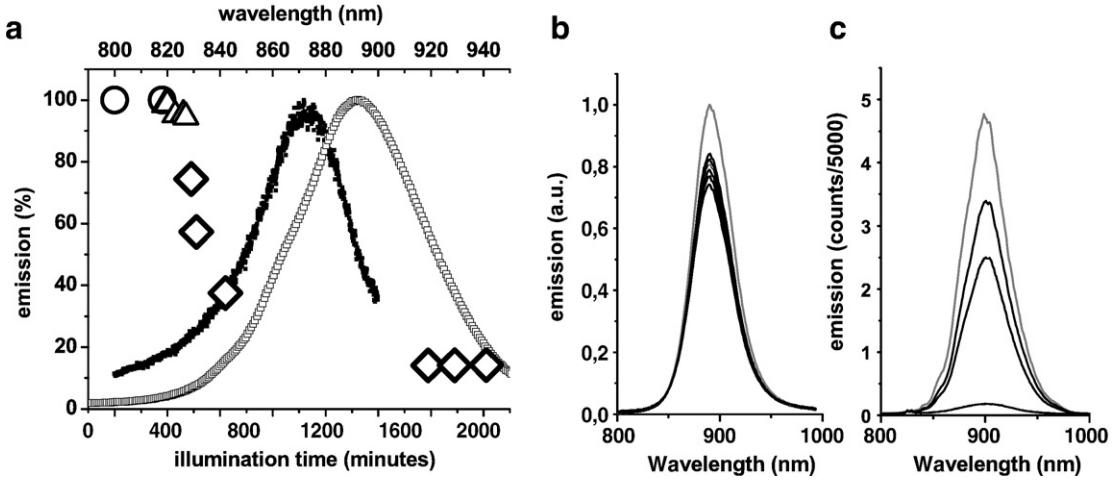

Fig. 5. Photoactivity of LH1 in solution and adsorbed onto gold. (a) Purified LH1 on gold: fluorescence excitation (black square) spectrum in vacuum and emission spectrum (open square spectrum in vacuum) and emission counts (circles, triangles and diamonds) at maximum in air. Power for excitation and emission spectra in vacuum 150 W cm^{-2}. Emission counts obtained in air with illumination power of 73 W cm^{-2}, in between emission measurements light-irradiation powers were employed of 73 W cm^{-2} (circles), 647 W cm^{-2} (triangles), and 228 kW cm^{-2} (diamonds). (b) LH1 in solution; emission spectra before (grey curve) and during (black curves) continuous white light illumination: Lowest curve obtained after 3 h. Emission spectra obtained by broad excitation: 400–600 nm. (c) LH1 in PVA spincoated on gold: consecutive confocal fluorescence emission spectra before (grey curve) and after removing the vacuum (black curves). Excitation at 825 nm, time between each spectrum is 60 s.

For comparison we also investigated purified WT-LH1 complexes in polyvinylalcohol, PVA, the preferred matrix for single-molecule experiments on photosynthetic complexes [23–25], spincoated onto a gold surface. Consecutive confocal fluorescence emission spectra of such preparation are shown in Fig. 5c, obtained at 60 s intervals. The initial emission spectrum displays an 8 nm red-shifted maximum compared to a solution spectra or gold-adsorbed LH1 (Fig. 5a). Strikingly, upon release of the vacuum the emission vanishes rapidly. Apparently, the photostability of LH1 under aerobic conditions is lost in the PVA matrix. PVA provides a dehydrated and rigid environment for LH1 that may induce structural distortions. AFM images of LH1 complexes showed large variations in shape attributed to the intrinsic flexibility of the circular LH1 proteins [26]. Our data here indicates that PVA acts upon this flexibility leading to structural deformations, resulting in a reduced photoactivity when exposed to air.

3.5. The function of LH2 and LH1 within membranes

Summarizing our results: we have shown that untreated, native chromatophores adsorb onto gold, and open up to form single membrane patches, while maintaining their primary photoconversion function. Photocurrent generation and energy transfer are also retained under aerobic conditions. We found different contributions to the functioning of these membranes for the light-harvesting complexes LH2 and LH1. An important clue about these differences was obtained by comparing the photocurrent generation of RC-LH1-only mutant with that of native WT membranes. Where LH1 absorption can contribute fully to the photocurrent, LH2-born excitations were already partially inactive at the lowest light intensities applicable and more strongly upon increased light intensities. Concomitantly, applying confocal fluorescence spectroscopy we found an increased emission for the LH2 component within the membranes upon increasing the light intensity. This suggests a reduced energy transfer from LH2→LH1 accounting for a decreased fluorescence excitation signal. Whereas isolated LH2 complexes photobleach immediately under ambient conditions, in native membranes LH2 only shuts down after high intensity irradiation. In contrast, isolated as well as membrane-embedded LH1 remained largely functional under the same conditions. From these observations we conclude firstly that within a network LH2 remains largely photostable. This is most likely due to the strongly reduced excited-state lifetime which reduces the probability of triplet state formation. Secondly, that at moderate light intensities the contribution of the LH2 complex to electron transfer is diminished. And thirdly, in comparison to LH2 the photostability of LH1 complexes proved to be extremely high. Likely it is this feature of LH1 that is responsible for the efficient functioning of the membranes under aerobic conditions. It is tempting to relate these effects to physiological conditions. Within an aqueous environment bacteria will reside at optimum light intensity. But these may change over time, in dim light LH2 is synthesised to increase light absorption [27], but becomes superfluous when light intensity increases. Our data indicates three energy dissipating mechanisms: firstly, at low-light, LH2 becomes reversibly decoupled from photocurrent generation. Secondly, at intermediate light we observed an increase in emission radiation, leading to less excitation transfer towards LH1 and ultimately the RCs. Unlike the former, this process is not immediately reversible. Last, at high light LH2 shuts down completely. Obviously, some mechanism must exist to largely prevent the same effects to occur in LH1 because this would deplete the bacterium completely from energy. Indeed our data indicate that LH1 is designed to remain largely functional, also when exposed to air, even under the harshest illumination conditions. We can only speculate about the possible causes for LH1 stability. Despite the similarity in the protein models of LH2 and LH1 significant differences must exist. There may be differences in carotenoid content [28]. Carotenoids are also known to stabilise protein complexes, thus more carotenoids in LH1 would also make this complex more robust. But the main role of carotenoids is to prevent the BChl pigments from photo-oxidation via triplet exchange or singlet oxygen quenching [29]. Both processes depend on the electronic structures of the BChl and carotenoids, the distances between them and the amount of carotenoids present, all yet unknown for LH1. The only other photosynthetic protein complex that has been shown to withstand photobleaching (up to 10 μW) when exposed to air is the peridinin–chlorophyll complex, or PCP that primarily consists of carotenoids [30]. We showed that dissolving LH1 within a rigid PVA matrix removes this complex ability to function under aerobic conditions, likely by inducing structural deformations. Since these distortions cannot be short-range or specific, we speculate that the strong photoprotection of LH1 described here lies within a specific arrangement of each BChl-car unit within the ring of proteins.

4. Conclusion

Our work has demonstrated for the first time the possibility of interfacing native photosynthetic assemblies onto a gold surface whilst retaining their optical activity and energy transforming capabilities. The native membranes are shown to be functional under aerobic conditions and withstanding illumination powers as high as direct solar irradiation. Illuminating native membranes adsorbed onto a gold-electrode show the highest photocurrents generated to date and demonstrated a remarkable durability. The light-harvesting complexes have been shown to dissipate excess energy through decoupling, increasing emission radiation and photobleaching. In contrast to isolated LH2 complexes, isolated LH1 complexes do not photobleach instantaneously under aerobic light conditions. We propose it is this robustness of the component linking energy- and electron transfers that allows photosynthesis to be largely retained in air, on a conducting surface and irradiated with high light. Our methodology presents a new way for detailed characterization of primary reactions of supramolecular light energy transducing assemblies.

Acknowledgements

The authors wish to thank Dre de Wit for growing the WT *R. sphaeroides* cells and isolating the chromatophores. This work was supported by grants to C.N.H. from the BBSRC (UK). R.N.F. gratefully acknowledges the Dutch Science Foundation NWO for a Veni-grant.

References

[1] G.R. Fleming, R. van Grondelle, The primary steps of photosynthesis, Physics Today 47 (1994) 48–55.
[2] J.N. Sturgis, J.D. Tucker, J.D. Olsen, C.N. Hunter, R.A. Niederman, Atomic force microscopic studies of native photosynthetic membranes, Biochemistry 48 (17) (2009) 3679–3698.
[3] R.J. Cogdell, P.K. Fyfe, S.J. Barret, S.M. Prince, A.A. Freer, N.W. Isaacs, P. McGlynn, C.N. Hunter, The purple bacterial photosynthetic unit, Photosynth. Res. 48 (1996) 55–63.
[4] C.N. Hunter, J.D. Pennoyer, R.A. Niederman, Assembly and structural organization of pigment–protein complexes in membranes of *Rhodopseudomonas sphaeroides*, Prog. Clin. Biol. Res. 102 (B) (1982) 257–265.
[5] R.N. Frese, C.A. Siebert, R.A. Niederman, C.N. Hunter, C. Otto, R. van Grondelle, The long-range organization of a native photosynthetic membrane, Proc. Natl. Acad. of Sci. U. S. A. 101 (2004) 17994–17999.
[6] S. Bahatyrova, R.N. Frese, C.A. Siebert, J.D. Olsen, K.O. Van der Werf, R. van Grondelle, R.A. Niederman, P.A. Bullough, C. Otto, C.N. Hunter, The native architecture of a photosynthetic membrane, Nature 430 (2004) 1058–1062.
[7] C. Jungas, J.-L. Ranck, J.-L. Rigaud, P. Joliot, A. Verméglio, Supramolecular organization of the photosynthetic apparatus of *Rhodobacter sphaeroides*, EMBO J. 18 (1999) 534–542.
[8] R.N. Frese, J.D. Olsen, R. Branvall, W.H.J. Westerhuis, C.N. Hunter, R. van Grondelle, The long-range supraorganization of the bacterial photosynthetic unit: a key role for PufX, Proc. Natl. Acad. U. S. A. 97 (2000) 5197–5202.
[9] C.A. Siebert, P. Qian, D. Fotiadis, A. Engel, C.N. Hunter, P.A. Bullough, Molecular architecture of photosynthetic membranes in *Rhodobacter sphaeroides*: the role of PufX, EMBO J. 23 (2004) 690–700.
[10] P. Qian, P.A. Bullough, C.N. Hunter, Three-dimensional reconstruction of a membrane-bending complex—The RC-LH1-PufX core dimer of *Rhodobacter sphaeroides*, J. Biol. Chem. 283 (2008) 14002–14011.

[11] M.K. Sener, J.D. Olsen, C.N. Hunter, K. Schulten, Atomic-level structural and functional model of a bacterial photosynthetic membrane vesicle, Proc. Natl. Acad. Sci. U. S. A. 104 (2007) 15723–15728.
[12] R.N. Frese, J.C. Pàmies, J.D. Olsen, S. Bahatyrova, C.D. van der Weij-de Wit, T.J. Aartsma, C. Otto, C.N. Hunter, D. Frenkel, R. van Grondelle, Protein shape and crowding drive domain formation and curvature in biological membranes, Biophys. J. 94 (2008) 640–647.
[13] S.M. Nie, R.N. Zare, Optical detection of single molecules, Ann. Rev. Biophys. Biomol. Struct. 26 (1997) 567–596.
[14] R. Guidelli, New directions and challenges in electrochemistry: bioelectrochemistry at metal–water interfaces, J. Electroanal. Chem. 504 (2001) 1–28.
[15] Y. Lu, J. Xu, B. Liu, J. Kong, Photosynthetic reaction center functionalized nanocomposite films: effective strategies for probing and exploiting the photo-induced electron transfer of photosensitive membrane protein, Biosens. Bioelec. 22 (2007) 1173–1185.
[16] S.A. Trammell, et al., Effect of protein orientation on electron transfer between photosynthetic reaction centers and carbon electrodes, Biosens. and Bioelec. 21 (2006) 1023–1028.
[17] N. Lebedev, et al., Conductive wiring of immobilized photosynthetic reaction center to electrode by cytochrome *c*, J. Am. Chem. Soc. 128 (2006) 12044–12045.
[18] Y. Suemori, et al., Self-assembled monolayer of light-harvesting core complexes of photosynthetic bacteria on an amino-terminated ITO electrode, Photosynth. res. 90 (2006) 17–21.
[19] M. Kondo, Y. Nakamura, K. Fuji, M. Nagata, Y. Suemori, T. Dewa, K. Lida, A.T. Gardiner, R.J. Cogdell, M. Nango, Self-assembled monolayer of light-harvesting core complexes from photosynthetic bacteria on a gold electrode modified with alkanethiols, Biomacromolcules 8 (2007) 2457–2463.
[20] P.M. Fraker, S. Kaplan, Isolation and fractionation of the photosynthetic membranous organelles from *Rhodopseudomonas spheroides*, J. Bacteriol. 108 (1971) 465–473.
[21] S. Weiss, Fluorescence spectroscopy of single biomolecules, Science 283 (1999) 1676–1683.
[22] M.A. Bopp, A. Sytnik, T.D. Howard, R.J. Cogdell, R.M. Hochstrasser, The dynamics of structural deformations of immobilized light-harvesting complexes, Proc. Natl. Acad. Sci. U. S. A. 96 (1999) 11271–11276.
[23] A.M. Van Oijen, M. Ketelaars, J. Köhler, T.J. Aartsma, J. Schmidt, Unraveling the electronic structure of individual pigment–protein complexes, Science 285 (1999) 400–402.
[24] C. Hofmann, T.J. Aartsma, H. Michel, J. Köhler, Direct observation of tiers in the energy landscape of a chromoprotein: a single-molecule study, Proc. Natl. Acad. Sci. U. S. A. 100 (26) (2003) 15534–15538.
[25] M.F. Richter, et al. Refinement of the X-ray structure of the RC-LH1 core complex from *Rhodopseudomonas palustris* by single-molecule spectroscopy. Proc. Nat. Acad. Sci. USA 104 (51) (2007) 20280-20284.
[26] S. Bahatyrova, R.N. Frese, K.O. van der Werf, C. Otto, C.N. Hunter, J.D. Olsen, Flexibility and size heterogeneity of the LH1 light harvesting complex revealed by atomic force microscopy: functional significance for bacterial photosynthesis, J. Biol. Chem. 279 (2004) 21327–21333.
[27] J. Aagaard, W.R. Sistrom, Control of synthesis of reaction center bacteriochlorophyll in photosynthetic bacteria, Photochem. Photobiol. 15 (1972) 209–225.
[28] C.N. Hunter, J.D. Pennoyer, J.N. Sturgis, D. Farrelly, R.A. Niederman, Oligomerization states and associations of light-harvesting pigment–protein complexes of *Rhodobacter sphaeroides* as analyzed by lithium dodecyl sulfate-polyacrylamide gel electrophoresis, Biochemistry 27 (1988) 3459–3467.
[29] R.J. Cogdell, A. Gall, J. Köhler, The architecture and function of the light-harvesting apparatus of purple bacteria: from single molecules to in vivo membranes, Quarter. Rev. Biophys. 39 (3) (2006) 227–324.
[30] S. Wörmke, et al., Single molecule fluorescence of native and refolded peridinin–chlorophyll–protein complexes, J. Fluoresc. 18 (2008) 611–617.